Chemistry of Mononuclear and Binuclear Oxidic V^V, V^VV^V, and V^VV^{IV} Azophenolates

Somnath Dutta, Partha Basu, and Animesh Chakravorty*

Department of Inorganic Chemistry, Indian Association for the Cultivation of Science, Calcutta 700032, India

*Received April 15, 1993**

The aerial reaction of 2,2′-dihydroxyazobenzene (H_2L) with bis(acetylacetonato)oxovanadium(IV) in methanol affords binuclear $V^V_2O_3L_2$. In the presence of KOH, $KV^VO_2L\cdot1.5H_2O$ is isolated. Dilute acids convert VO_2L^- to $V_2O_3L_2$ via $V^VO(OH)L$. The electronic and IR spectra of the complexes are described. In crystalline $KVO_2L\cdot1.5H_2O$, the vanadium(V) atom has square pyramidal geometry. The base is formed by coordinated ONO atoms of L^{2-} and an oxo oxygen atom. The metal atom is displaced by ~0.5 Å from the base toward the apical oxo oxygen atom. The O–V–O angle is >107°, which is a characteristic feature of VO_2^+ complexes with pentacoordinated vanadium. The VO_2L^- units are interlinked into an infinite network by K^+ ions (bonded to water, oxo, and phenolic oxygen atoms). In crystalline $V_2O_3L_2$, two VOL fragments are bridged by an oxygen atom lying on a 2-fold axis. The geometry of the pentacoordinated metal atom is similar to that in VO_2L^-, the bridging oxygen atom defining the shared corner of the bases of the two metal pyramids. The two terminal oxygen atoms are trans-directed lying on opposite sides of the VOV plane. The V–O(phenolic) length in $V_2O_3L_2$ is shorter than that in $KVO_2L\cdot1.5H_2O$ by ~0.1 Å due to stronger metal–phenol π-bonding in the former complex. Crystal data for $KVO_2L\cdot1.5H_2O$: monoclinic; space group $C2/c$; a = 33.834(9) Å, b = 7.245(2) Å, c = 23.708(4) Å; β = 103.56(2)°; V = 5649(2) Å^3; Z = 16; R = 3.64%; R_w = 4.07%. Crystal data for $V_2O_3L_2$: orthorhombic; space group $Pcnb$; a = 7.392(2) Å, b = 12.868(2) Å, c = 24.371(7) Å; V = 2318(1) Å^3; Z = 4; R = 3.84%, R_w = 4.38%. In dichloromethane solution this complex displays a one-electron couple, $V_2O_3L_2$–$V_2O_3L_2^-$, having an $E_{1/2}$ value of 0.30 V vs SCE. The electrogenerated mixed-valence (V^VV^{IV}) complex $V_2O_3L_2^-$ shows intervalence bands at 760 and 980 nm. At room temperature its solution (1.77 μ_B) EPR spectrum consists of 15 lines (A = 49.9 G; g = 1.98) corresponding to the delocalization of the unpaired electron over the two equivalent metal atoms. In frozen glass (77 K) the electron is localized at one center ($A_\parallel$ = 174.3 G, $A_\perp$ = 64.2 G; $g_\parallel$ = 1.96; $g_\perp$ = 1.98). From variable-temperature EPR spectra the activation energy and rate constant (298 K) for the delocalization process are estimated to be 3.1 kcal mol^{-1} and 3.2 × 10^{10} s^{-1}, respectively.

Introduction

This work forms part of a study on the synthesis, characterization, and reactivity of oxo–vanadium complexes incorporating oxygen and nitrogen donor ligands.[1] Herein we explore the binding of the diphenolic azo ligand **1**, abbreviated H_2L.[2] Dioxidic

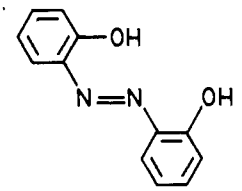

1 H_2L

mononuclear and trioxidic binuclear vanadium(V) species have been isolated, structurally characterized, and scanned for metal-centered electroactivity. Noteworthy features include the following. The vanadium atoms in the complexes are uniformly pentacoordinated—a relatively uncommon situation for the oxidic pentavalent state. The V–O(phenolic) bond order and the vanadium(V)–vanadium(IV) reduction potential increase considerably in going from the mononuclear to the binuclear stage. Upon electroreduction, the latter affords the mixed-valence (V^VV^{IV}) analog in solution. The unpaired electron is delocalized over both metal atoms, but it can be trapped at one center by cooling. The activation energy for this phenomenon observed for the first time for an oxidic divanadium core has been estimated. As vanadium phenolates, the present complexes are also of peripheral bioinorganic interest.[3-7]

Results and Discussion

Synthesis and Spectra. The synthesis of complexes is summarized in Scheme I. The smooth displacement of acetylacetone (Hacac) by H_2L from $VO(acac)_2$ occurs with concomitant aerial oxidation[8] of the metal, affording $V_2O_3L_2$. In the presence of alkali the mononuclear anion VO_2L^- results. Dilute acid quantitatively transforms VO_2L^- to $V_2O_3L_2$, probably via the protonated[9-11] form VO(OH)L. The latter has been isolated and shown to undergo spontaneous self-condensation to $V_2O_3L_2$ upon standing in solution (Scheme I). The complex $KVO_2L\cdot1.5H_2O$ behaves as a 1:1 electrolyte in solution (Λ = 113 Ω^{-1} cm^2 M^{-1} in MeCN).

* Abstract published in *Advance ACS Abstracts*, October 1, 1993.

(1) Earlier publication: Basu, P.; Pal, S.; Chakravorty, A. *J. Chem. Soc., Dalton Trans.* **1991**, 3217–3221.
(2) Manganese(IV) complexes: Dutta, S.; Basu, P.; Chakravorty, A. *Inorg. Chem.* **1991**, *30*, 4031–4037.
(3) Rehder, D. *Angew. Chem., Int. Ed. Engl.* **1991**, *30*, 148–167.
(4) Butler, A.; Carrano, C. J. *Coord. Chem. Rev.* **1991**, *109*, 61–105.
(5) (a) Wever, R.; Kustin, K. *Adv. Inorg. Chem.* **1990**, *35*, 81–115. (b) Kustin, K.; McLeod, G. C.; Gilbert, T. R.; Briggs, L. B. R., IV. *Struct. Bonding (Berlin)* **1983**, *53*, 139–160.
(6) Chasteen, N. D. *Struct. Bonding (Berlin)* **1983**, *53*, 105–138.
(7) Chasteen, N. D. *Vanadium in Biological Systems*; Kluwer Academic Publishers: Dordrecht, The Netherlands, 1990.
(8) In the absence of air an antiferromagnetic (1.55 μ_B at 296 K) complex of approximate composition $[VOL]_n$ is formed. Solutions of $[VOL]_n$ undergo facile oxidation in air, affording $V_2O_3L_2$. We have not been able to fully characterize $[VOL]_n$ or to grow single crystals of it, but its structure may be similar to those proposed for certain binuclear salicylaldimines, as in: Ginsberg, A. P.; Koubeck, E.; Williams, H. J. *Inorg. Chem.* **1966**, *5*, 1656–1662.
(9) Giacomelli, A.; Floriani, C.; Duarte, A. O. D. S.; Chiesi-Villa, A.; Guastiani, C. *Inorg. Chem.* **1982**, *21*, 3310–3316.
(10) Bonadies, J. A.; Carrano, C. J. *J. Am. Chem. Soc.* **1986**, *108*, 4088–4095.
(11) Knopp, P.; Wieghardt, K.; Nuber, B.; Weiss, J.; Sheldrick, W. S. *Inorg. Chem.* **1990**, *29*, 363–371.

0020-1669/93/1332-5343$04.00/0

Scheme I[a]

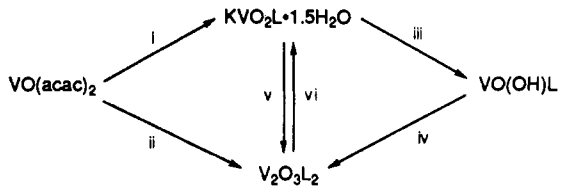

[a] Key: (i) 1 mol of H_2L; 2 mol of KOH; MeOH; stir. (ii) 1 mol of H_2L; MeOH; stir. (iii) HCl(g); CH_3CN; stir. (iv) Let stand in CH_2Cl_2. (v) 1 mol of HCl or $HClO_4$; water; stir. (vi) 2 mol of KOH; MeOH; stir.

Table I. Electronic and IR Spectral Data

complex	UV–vis λ_{max}, nm (ϵ, M^{-1} cm^{-1})	V–O str,[e] cm^{-1}
$KVO_2L·1.5H_2O$[a]	480 (9750), 430[d] (6080), 320 (8390)	940, 920
$V_2O_3L_2$[b]	475 (15 680), 325 (36 650)	990, 775
VO(OH)L[b]	520[d] (1990), 420[d] (6020), 380[d] (6620), 320 (9400)	990
$V_2O_3L_2^-$[c]	980 (500), 760 (590), 490 (18 360), 325 (21 250)	

[a] In CH_3CN. [b] In CH_2Cl_2. [c] Electrogenerated in CH_2Cl_2 solution. [d] Shoulder. [e] In KBr disks.

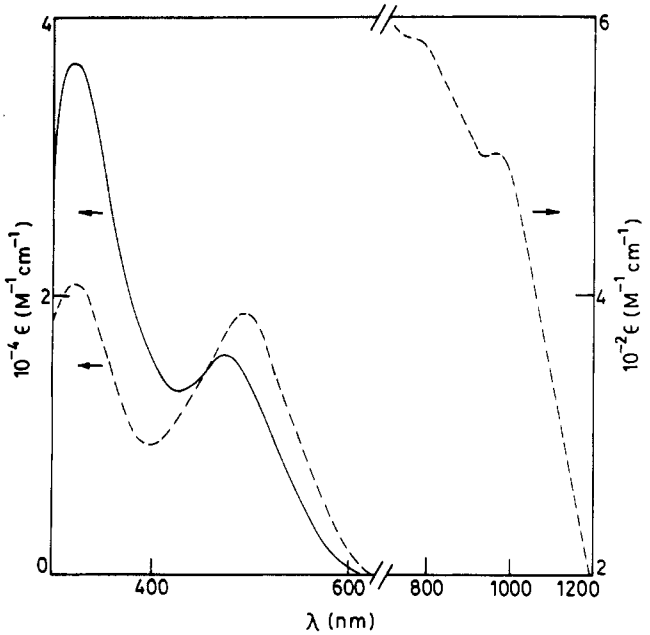

Figure 1. Electronic spectra of $V_2O_3L_2$ (—) and electrogenerated $V_2O_3L_2^-$ (- - -) in dichloromethane solution at 298 K.

Selected spectral data are collected in Table I. The V–O stretching modes[10,12] are observed in the region 750–1000 cm^{-1}—the VO_2^+ and $V_2O_3^{4+}$ moieties having two stretches each. The electronic spectra of the vanadium(V) complexes consist of several bands in the region 300–550 nm. The band system near 450 nm is believed to be of the $L^{2-} \rightarrow V^V$ charge-transfer type. The spectra of $V_2O_3L_2$ and its electroreduced congener $V_2O_3L_2^-$ displaying intervalence bands (*vide infra*) are compared in Figure 1. The ^1H NMR spectrum of VO(OH)L in $CDCl_3$ has a sharp signal of correct intensity at δ 12.30 due to the OH function (disappears upon shaking with D_2O).

Structures. a. $KVO_2L·1.5H_2O$. Two structurally very similar but crystallographically distinct VO_2L^- anions are present (Figure 2). The L^{2-} ligands of the two molecules lie nearly parallel to each other (dihedral angle 5.6°), the distance between their centroids being 4.890 Å. Selected bond parameters are listed in Table II. The lattice has an infinite network of V–O··K (bridging

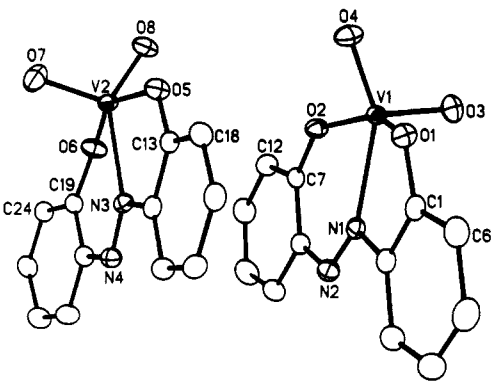

Figure 2. ORTEP plot and atom-labeling scheme for the VO_2L^- pair in $KVO_2L·1.5H_2O$. All non-hydrogen atoms are represented by their 30% probability ellipsoids.

Table II. Selected Bond Distances (Å) and Angles (deg) in $KVO_2L·1.5H_2O$

Distances			
V(1)–O(1)	1.953(2)	V(1)–O(2)	1.912(2)
V(1)–O(3)	1.625(2)	V(1)–O(4)	1.637(2)
V(1)–N(1)	2.205(3)	V(2)–O(5)	1.956(2)
V(2)–O(6)	1.914(2)	V(2)–O(7)	1.612(3)
V(2)–O(8)	1.643(2)	V(2)–N(3)	2.208(3)
K(1)–O(2)	2.745(2)	K(1)–O(4)	2.783(3)
K(1)–O(5)	2.816(3)	K(1)–O(8)	2.806(2)
K(1)–O(1w)	2.768(3)	K(1)–O(2w)	2.861(3)
K(1)–O(4a)[a]	2.719(2)	K(2)–O(8)	2.916(3)
K(2)–O(3w)	2.880(3)	K(2)–O(7a)[b]	2.846(3)
K(2)–O(1wa)[b]	2.804(2)	K(2)–O(2wa)[b]	2.940(3)
K(2)–O(3wa)[b]	2.743(3)	O(1)–C(1)	1.341(4)
O(2)–C(7)	1.318(3)	O(5)–C(13)	1.345(4)
O(6)–C(19)	1.329(3)	N(1)–N(2)	1.269(3)
N(3)–N(4)	1.269(3)		
Angles			
O(1)–V(1)–O(2)	148.8(1)	O(1)–V(1)–O(3)	100.1(1)
O(2)–V(1)–O(3)	105.8(1)	O(1)–V(1)–O(4)	93.7(1)
O(2)–V(1)–O(4)	94.6(1)	O(3)–V(1)–O(4)	107.8(1)
O(1)–V(1)–N(1)	76.3(1)	O(2)–V(1)–N(1)	80.1(1)
O(3)–V(1)–N(1)	105.9(1)	O(4)–V(1)–N(1)	146.6(1)
O(5)–V(2)–O(6)	150.5(1)	O(5)–V(2)–O(7)	102.7(1)
O(6)–V(2)–O(7)	101.8(1)	O(5)–V(2)–O(8)	93.7(1)
O(6)–V(2)–O(8)	93.7(1)	O(7)–V(2)–O(8)	109.1(1)
O(5)–V(2)–N(3)	75.8(1)	O(6)–V(2)–N(3)	80.6(1)
O(7)–V(2)–N(3)	109.6(1)	O(8)–V(2)–N(3)	141.3(1)

[a] Coordinates of O(4a): $\bar{x} + 1/2, \bar{y} + 3/2, \bar{z}$. [b] Coordinates of O(7a), O(1wa), O(2wa), O(3wa): $\bar{x} + 1/2, \bar{y} + 1/2, \bar{z} + 1/2$.

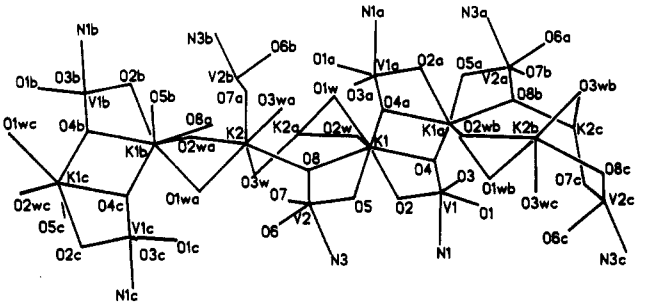

Figure 3. Views of the V–O··K and K··O··K network in crystalline $KVO_2L·1.5H_2O$.

oxygen being oxo and phenolic) and K··O··K (oxo and water) linkages (Figure 3). There are seven and six <3-Å K··O contacts for K(1) and K(2), respectively (Table II). Solution electrical conductivity data (*vide supra*) reveal that the above type of ionic association is essentially absent in acetonitrile solution.

The coordination geometry of the VO_2L^- anion is distorted square pyramidal. The base is defined by the coordinated ONO atoms of the planar (mean deviation ~0.06 Å) L^{2-} ligand and an oxo oxygen atom. The other oxo oxygen atom (O(3) for V(1)

(12) Toftlund, H.; Larsen, S.; Murray, K. S. *Inorg. Chem.* **1991**, *30*, 3964–3967.

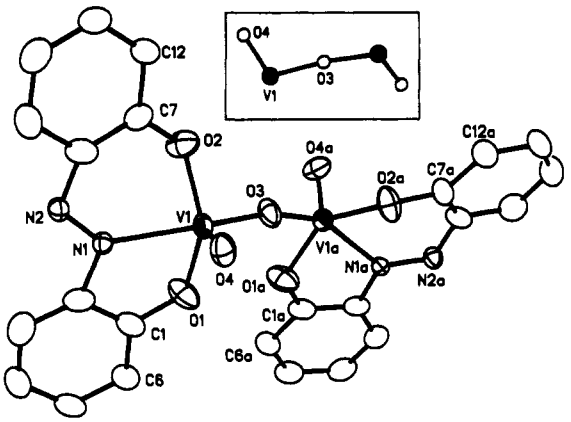

Figure 4. ORTEP plot and atom-labeling scheme for $V_2O_3L_2$. All non-hydrogen atoms are represented by their 30% probability ellipsoids. The relative orientation of the two terminal oxygen atoms is shown in the inset.

Table III. Selected Bond Distances (Å) and Angles (deg) in $V_2O_3L_2$

		Distances	
V(1)–O(1)	1.851(3)	V(1)–O(2)	1.832(3)
V(1)–O(3)	1.770(1)	V(1)–O(4)	1.574(3)
V(1)–N(1)	2.165(7)	C(1)–O(1)	1.340(5)
C(7)–O(2)	1.330(5)	N(1)–N(2)	1.294(9)
		Angles	
O(1)–V(1)–O(2)	142.6(2)	O(1)–V(1)–O(3)	93.1(2)
O(2)–V(1)–O(3)	95.4(1)	O(1)–V(1)–O(4)	106.7(2)
O(2)–V(1)–O(4)	104.9(1)	O(3)–V(1)–O(4)	108.6(1)
O(1)–V(1)–N(1)	71.8(2)	O(2)–V(1)–N(1)	85.5(2)
O(3)–V(1)–N(1)	154.2(2)	O(4)–V(1)–N(1)	96.0(2)
V(1)–O(3)–V(1a)	160.8(2)		

and O(7) for V(2)) occupy the apex of the pyramid. The metal atom is displaced from the base toward the apical oxygen atom by 0.486 Å for V(1) and 0.509 Å for V(2). The V–O(oxo) distances lie in the range 1.612(3)–1.643(2) Å, the apical distances being slightly shorter than the basal distance in each anion.

In most structurally characterized complexes of VO_2^+, the metal atom is hexacoordinated with distorted octahedral geometry.[13-20] In general, V–O(oxo) distances (usual span 1.61–1.65 Å) for VO_2^+ complexes are not discriminatory of the metal coordination number but the O–V–O angle appears to be so. In virtually all the known structures of hexacoordinated complexes,[13-17] this angle is <107° while that in the known pentacoordinated species[18-20] is invariably >107°. The angles in $KVO_2L\cdot1.5H_2O$, 107.8(1) and 109.1(1)°, are in line with this pattern.

b. $V_2O_3L_2$. Discrete molecules (Figure 4) constitute the crystal lattice with the bridging oxygen atom lying on a crystallographic 2-fold axis. Bond parameters are given in Table III. The geometry of the metal atom is similar to that in VO_2L^-, but here the pyramid base is constituted of ONO of L^{2-} and the bridging oxygen atom O(3). The metal is displaced toward the oxo apex, O(4), by 0.470 Å. The dihedral angle between the pyramid bases corresponding to V(1) and V(1a) is 36.5°. The two terminal oxygen atoms, O(4) and O(4a), are trans-directed lying on opposite sides of the VOV plane (inset in Figure 4). The distance of each oxygen atom from the plane is 1.380 Å. The O(4a)V(1a)-V(1)O(4) torsion angle is 142.0°.

Bond distances within the coordination spheres of $V_2O_3L_2$ and VO_2L^- are compared in **2** (average values) and **3**. Meaning of

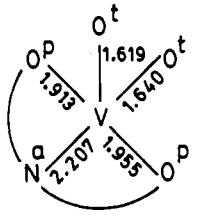

VO_2L^-

2

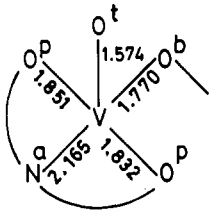

$V_2O_3L_2$

3

superscripts on the oxygen atoms: t = terminal, b = bridging, p = phenolic, a = azo. The V–O^t length in **3** is slightly shorter than that in **2**, but V–O^b is much longer than V–O^t. As a result, the V–N^a length in **2** (trans to V–O^t) is significantly longer than that in **3** (trans to V–O^b). Further, the V–O^p lengths follow the order **3** < **2**. Indeed, the difference between the average V–O^p lengths of **2** and **3** is a remarkable ~0.1 Å. This is believed to arise largely from augmentation of V–O^p π-bonding ($O^p \rightarrow V$ sense) in **3** in order to compensate for the weaker (compared to V–O^t in **2**) V–O^b π-bonding. Interestingly, the simple average of all V–O distances in **2** is 1.78 Å, close to that in **3**, 1.76 Å.

The structures of four other complexes of $V_2O_3^{4+}$ are known.[21-24] In one of these[24] the metal coordination numbers are 5 and 5 (as in $V_2O_3L_2$). In another[23] these are 5 and 6, and in the remaining two[21,22] they are 6 and 6. Among these complexes, the relative orientations of the two coordination spheres vary widely due to large variations in the V–O–V angle and the rotational disposition about the V–O^b bonds.[25]

Metal Redox: Mixed-valence $V_2O_3L_2^-$. The pentavalent state in VO_2L^- is strongly stabilized, and the complex is not electroactive in the voltage window ±1 V versus SEC (Pt electrode, MeCN solution).[26] Metal redox is expected[27] to be facilitated by protonation and indeed VO(OH)L shows a one-electron couple with $E_{1/2}$ = –0.05 V (peak-to-peak separation ΔE_p = 90 mV) in dichloromethane solution. The response is assigned to vanadium(V)–vanadium(IV) redox.

Formally $V_2O_3L_2$ is an analog of VO(OH)L with H^+ replaced by $[VOL]^+$, and it also shows a vanadium(V)–vanadium(IV) couple (eq 1) in dichloromethane solution.[26] The $E_{1/2}$ and ΔE_p values are respectivley 0.30 V and 120 mV. Constant-potential coulometry at 0.0 V leads to quantitative formation of the one-

(13) Li, X.; Lah, M. S.; Pecoraro, V. L. *Inorg. Chem.* **1988**, *27*, 4657–4664.
(14) Kojima, A.; Okazaki, K.; Ooi, S.; Saito, K. *Inorg. Chem.* **1983**, *22*, 1168–1174.
(15) (a) Scheidt, W. R.; Tsai, C.; Hoard, J. L. *J. Am. Chem. Soc.* **1971**, *93*, 3867–3872. (b) Scheidt, W. R.; Collins, D. M.; Hoard, J. L. *J. Am. Chem. Soc.* **1971**, *93*, 3873–3877. (c) Scheidt, W. R.; Countryman, R.; Hoard, J. L. *J. Am. Chem. Soc.* **1971**, *93*, 3878–3882.
(16) Drew, R. E.; Einstein, F. W. B.; Gransden, S. E. *Can. J. Chem.* **1974**, *52*, 2184–2189.
(17) Brand, S. G.; Edelstein, N.; Hawkins, C. J.; Shalimoff, G.; Snow, M. R.; Tiekink, E. R. T. *Inorg. Chem.* **1990**, *29*, 434–438.
(18) (a) Galesic, N.; Siroki, M. *Acta Crystallogr., Sect. B* **1979**, *35*, 2931–2937. (b) Galesic, N.; Siroki, M. *Acta Crystallogr., Sect. C* **1984**, *40*, 378–381.
(19) Nakajima, K.; Tokida, N.; Kojima, M.; Fujita, J. *Bull. Chem. Soc. Jpn.* **1992**, *65*, 1725–1727.
(20) Rieskamp, V. H.; Mattes, R. *Z. Anorg. Allg. Chem.* **1976**, *419*, 193–199.
(21) Yamada, S.; Katayama, C.; Tanaka, J.; Tanaka, M. *Inorg. Chem.* **1984**, *23*, 253–255.
(22) Nakajima, K.; Kojima, M.; Toriumi, K.; Saito, K.; Fujita, J. *Bull. Chem. Soc. Jpn.* **1989**, *62*, 760–767.
(23) Casellato, U.; Vigato, P. A.; Graziani, R.; Vidali, M.; Milani, F.; Musiani, M. M. *Inorg. Chim. Acta* **1982**, *61*, 121–128.
(24) Diamantis, A. A.; Fredereksen, J. M.; Salam, M. A.; Snow, M. R.; Tiekink, E. R. T. *Aust. J. Chem.* **1986**, *39*, 1081–1088.
(25) This can be visualized with the help of the following V–O–V angle and O^tVVO^t torsion angle data: 180 and 180° for $V_2O_3A_2$; 173.4(4) and 67.3° for $V_2O_3B_4$; 116.2(8), 141.1(10)° and 90.5, 66.7° for $[V_2O_3D_2]_2\cdot 2CH_2Cl_2$, which has two dissimilar molecules; 156(1) and 104.9° for $[V_2O_3E_2]_2$·dioxane (H_2A = 4-phenylbutane-2,4-dione benzoylhydrazone; HB = 8-quinolinol; H_2D = N-(methylcarboxymethyl)salicylideneamine; H_2E = *N*-(2-hydroxyphenyl)salicylideneamine). The torsion angles stated above were calculated from the reported coordinates.[21-24]
(26) Below –1 V, one or more reductions are observed, presumably due to the azo group. These responses are absent in the salicylaldimine analogs (unpublished results from this laboratory).
(27) Chakravorty, A. *Comments Inorg. Chem.* **1985**, *4*, 1–16.

$$V^{V}{}_2O_3L_2 + e^- \rightleftharpoons V^{V}V^{IV}O_3L_2^- \quad (1)$$

electron-reduced complex, and upon reoxidation at +0.6 V, $V_2O_3L_2$ is fully regenerated.

Attempted isolation of the reduced complex, $V_2O_3L_2^-$, in the form of pure salts has not been successful, but it has been characterized in solution with the help of electronic and EPR spectroscopy. The complex displays two moderately intense bands at 760 and 980 nm which are absent in $V_2O_3L_2$ (Figure 1, Table I). In view of the observations noted in the next section, these are logically assigned to intervalence charge-transfer transitions.

EPR Spectra: Valence Delocalization in $V_2O_3L_2^-$. The magnetic moment of $V_2O_3L_2^-$ in dichloromethane solution is 1.77 μ_B, corresponding to the presence of one unpaired electron. The room-temperature EPR spectrum of electrogenerated $V_2O_3L_2^-$ in dichloromethane solution consist of 15 lines (Figure 5). The values of the isotropic coupling constant (A) and the g factor are 49.9 G and 1.98, respectively. In contrast, the spectrum (Figure 5) in the glassy state at 77 K has parallel and perpendicular lines characteristic of isolated axial $V^{IV}O$ centers[1,28] with $g_\parallel < g_\perp$ and $A_\parallel > A_\perp$. The relevant parameters are $g_\parallel = 1.96$, $g_\perp = 1.98$, $g_{av} = 1.97$, $A_\parallel = 174.3$ G, $A_\parallel = 64.2$ G, and $A_{av} = 100.9$ G.

At room temperature the unpaired electron is delocalized over two equivalent metal atoms (^{51}V, $I = {}^7/_2$) which behave as if there were one interacting nucleus with a total nuclear spin of 7. At 77 K the unpaired electron is localized at a single center interacting with only one ^{51}V nucleus. A diagnostic feature of such a situation is the doubling of the hyperfine coupling constant in going to the localized state.[29] For $V_2O_3L_2^-$ we indeed have $A \approx 0.5A_{av}$.

The rate constant (k_r) and activation energy (ΔE_a) for the localized → delocalized transformation have been estimated from variable-temperature (300-77 K) EPR spectra using a procedure that has been utilized earlier in the case of certain $Cu^{II}Cu^{I}$ species.[30,31] Spectra at a few selected temperatures are shown in Figure 6. Only the central portion is displayed, since the outer lines become ill-defined upon cooling due to broadening.

At 190 K the spectrum still retains the features of delocalization ($A \sim 50$ G), but just below the freezing point of the solvent (176 K) the axial spectrum of the localized state becomes discernible. It is estimated that the coalescence temperature is ~180 K. The lifetime (2τ) of the localized state at this temperature can be set equal to $\sqrt{2}/\pi A_{av}$ or 1.63×10^{-9} s, the corresponding rate constant ($k_r = {}^1/_{2\tau}$) being 6.14×10^8 s^{-1}. The activation energy (unit transmission coefficient assumed) computed with the help of the relation $k_r = (kT/h)\exp(-\Delta E_a/RT)$ is 3.1 kcal mol^{-1}. The value of k_r at 298 K is then 3.2×10^{10} s^{-1}.

To our knowledge, this represents the first demonstration and thermodynamic characterization of a thermally controllable valence delocalization phenomenon in an oxidic $V^{V}V^{IV}$ species. The EPR spectrum of an aqueous solution containing $[V^{IV}O(nta)(H_2O)]^-$ and an excess of $[V^{V}O_2(nta)]^{2-}$ consists of multiple lines assigned to be those due to $[V_2O_3(nta)_2]^{3-}$ and unreacted $[V^{IV}O(nta)(H_2O)]^-$ (nta = nitrotriacetate).[32] The X-ray structure of $(NH_4)_3[V_2O_3(nta)_2]\cdot 3H_2O$[32] and that of a related mixed-valence complex have been reported.[33] A $V^{V}V^{IV}$ complex based on 8-hydroxyquinoline with only ill-defined signs of valence delocalization has also been described.[34]

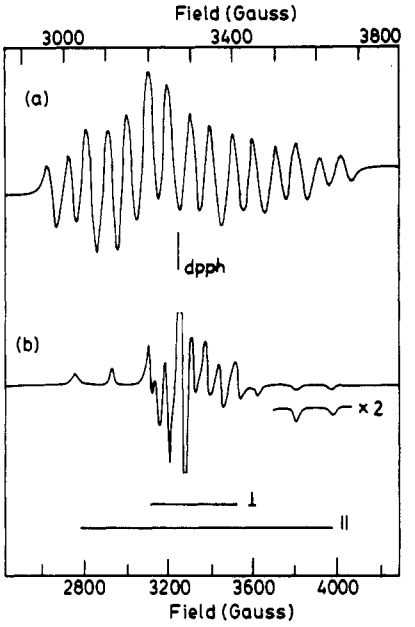

Figure 5. EPR spectra at X-band of $V_2O_3L_2^-$ electrogenerated in dichloromethane: (a) 298 K with sweep width 1000 G (top scale); (b) 77 K with sweep width 2000 G (bottom scale). Instrument settings: power, 30 dB; modulation, 100 kHz, sweep center, 3300 G; sweep time, 240 s.

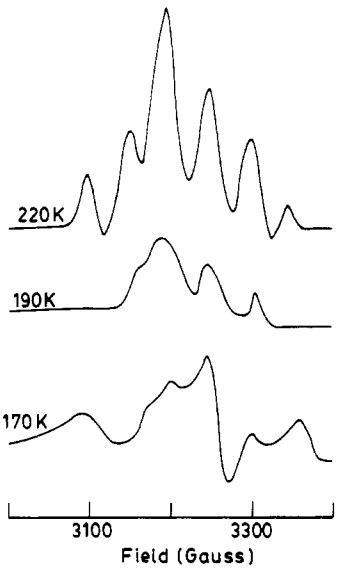

Figure 6. Variable-temperature EPR spectra of electrogenerated $V_2O_3L_2^-$ in dichloromethane solution. Instrument settings: power, 30 dB; modulation, 100 kHz; sweep center, 3250 G; sweep width, 1000 G; sweep time, 240 s.

Concluding Remarks

The main findings of this work and prospects of further activity will now be briefly stated. The tridentate ONO-coordinating diphenolic azo ligand H_2L has afforded pentacoordinated square pyramidal vanadium(V) species of mononuclear dioxidic and binuclear trioxidic types—VO_2L^- and $V_2O_3L_2$, both of which have been structurally characterized. The L^{2-} ligand is more tightly bound (stronger O→V π-bonding) to the metal at the phenolic oxygen atom in the latter than in the former complex.

Acids convert VO_2L^- to $V_2O_3L_2$ via $VO(OH)L$, and alkali reverses the transformation. The divanadium complex is re-

(28) Cornman, C. R.; Kampf, J.; Lah, M. S.; Pecoraro, V. L. *Inorg. Chem.* **1992**, *31*, 2035–2043.
(29) (a) Wertz, J. E.; Bolton, J. R. *Electron Spin Resonance*; McGraw-Hill: New York, 1972; p 210. (b) Pilbrow, J. R. *Transition Ion Electron Paramagnetic Resonance*; Clarendon Press: Oxford, U.K., 1990; p 339.
(30) Gagne, R. R.; Koval, C. A.; Smith, T. J.; Cimolino, M. C. *J. Am. Chem. Soc.* **1979**, *101*, 4571–4580.
(31) Long, R. C.; Hendrickson, D. N. *J. Am. Chem. Soc.* **1983**, *105*, 1513–1521.
(32) Nishizawa, M.; Hirotsu, K.; Ooi, S.; Saito, K. *J. Chem. Soc., Chem. Commun.* **1979**, 707–708.
(33) Kojima, A.; Okazaki, K.; Ooi, S.; Saito, K. *Inorg. Chem.* **1983**, *22*, 1168–1174.
(34) Riechel, T. L.; Sawyer, D. T. *Inorg. Chem.* **1975**, *14*, 1869–1875.

Table IV. Crystallographic Data for $KVO_2L\cdot1.5H_2O$ and $V_2O_3L_2$

	$KVO_2L\cdot1.5H_2O$	$V_2O_3L_2$
empirical formula	$C_{12}H_{11}N_2O_{5.5}KV$	$C_{24}H_{16}N_4O_7V_2$
fw	361.3	574.3
space group	$C2/c$	$Pcnb$
a, Å	33.834(9)	7.392(2)
b, Å	7.245(2)	12.868(2)
c, Å	23.708(4)	24.371(7)
β, deg	103.56(2)	
V, Å^3	5649(2)	2318(1)
Z	16	4
T, °C	22	22
λ, Å	0.710 73	0.710 73
ρ_{calcd}, g cm^{-3}	1.699	1.646
μ, cm^{-1}	10.23	8.61
transm coeff[a]	0.88/1	0.97/1
R,[b] %	3.64	3.84
R_w,[c] %	4.07	4.38
GOF[d]	1.42	1.02

[a] Maximum value normalized to 1. [b] $R = \sum\|F_o\| - |F_c\|/\sum|F_o|$. [c] $R_w = [\sum w(|F_o| - |F_c|)^2/\sum w|F_o|^2]^{1/2}$; $w^{-1} = \sigma^2(|F_o|) + g|F_o|^2$; $g = 0.0002$ for both $KVO_2L\cdot1.5H_2O$ and $V_2O_3L_2$. [d] The goodness of fit is defined as $[w(|F_o| - |F_c|)^2/(n_o - n_v)]^{1/2}$ where n_o and n_v denote the numbers of data and variables, respectively.

Table V. Atomic Coordinates (×10^4) and Equivalent[a] Isotropic Displacement Coefficients (Å^2 × 10^3) for $KVO_2L\cdot1.5H_2O$

	x	y	z	U(eq)
V(1)	3326(1)	5394(1)	-199(1)	23(1)
V(2)	3276(1)	8538(1)	2049(1)	27(1)
K(1)	2663(1)	6056(1)	789(1)	32(1)
K(2)	2475(1)	8230(1)	2850(1)	39(1)
O(1)	3455(1)	6866(3)	-821(1)	31(1)
O(2)	3401(1)	4942(3)	614(1)	31(1)
O(3)	3269(1)	3377(3)	-506(1)	38(1)
O(4)	2874(1)	6311(3)	-275(1)	38(1)
O(5)	3204(1)	8960(3)	1217(1)	36(1)
O(6)	3562(1)	7417(3)	2759(1)	37(1)
O(7)	3143(1)	10490(4)	2275(1)	50(1)
O(8)	2892(1)	7093(4)	1961(1)	40(1)
O(1W)	2001(1)	4896(3)	1194(1)	41(1)
O(2W)	2634(1)	2176(4)	999(1)	49(1)
O(3W)	2995(1)	5038(4)	3088(1)	48(1)
N(1)	3987(1)	5831(3)	89(1)	26(1)
N(2)	4252(1)	5493(4)	552(1)	32(1)
N(3)	3902(1)	8742(4)	1930(1)	29(1)
N(4)	4250(1)	8534(4)	2268(1)	32(1)
C(1)	3844(1)	7006(4)	-856(1)	27(1)
C(2)	4146(1)	6540(5)	-372(1)	29(1)
C(3)	4559(1)	6727(5)	-371(2)	37(1)
C(4)	4659(1)	7319(6)	-868(2)	46(1)
C(5)	4357(1)	7762(5)	-1363(2)	43(1)
C(6)	3950(1)	7629(5)	-1359(1)	35(1)
C(7)	3712(1)	4574(4)	1051(1)	26(1)
C(8)	4119(1)	4847(5)	1027(1)	28(1)
C(9)	4434(1)	4533(5)	1526(2)	39(1)
C(10)	4350(1)	3948(6)	2031(2)	45(1)
C(11)	3949(1)	3651(5)	2052(2)	42(1)
C(12)	3636(1)	3956(5)	1576(1)	34(1)
C(13)	3524(1)	9396(4)	995(1)	26(1)
C(14)	3911(1)	9283(4)	1357(1)	26(1)
C(15)	4253(1)	9721(5)	1156(1)	33(1)
C(16)	4208(1)	10252(5)	583(1)	33(1)
C(17)	3820(1)	10365(5)	219(1)	32(1)
C(18)	3481(1)	9945(5)	422(1)	32(1)
C(19)	3938(1)	7629(5)	3080(1)	28(1)
C(20)	4270(1)	8061(5)	2839(1)	29(1)
C(21)	4666(1)	8053(5)	3195(2)	37(1)
C(22)	4731(1)	7758(5)	3776(2)	40(1)
C(23)	4400(1)	7435(5)	4022(1)	35(1)
C(24)	4011(1)	7354(4)	3681(1)	32(1)

[a] Equivalent isotropic U defined as one-third of the trace of the orthogonalized U_{ij} tesor.

versibly electroreducible, affording the mixed-valence $V^{V}V^{IV}$ complex $V_2O_3L_2^-$ ($S = {}^1/_2$) in solution. Localization of the unpaired electron at a single metal center occurs below 180 K,

Table VI. Atomic Coordinates (×10^4) and Equivalent[a] Isotropic Displacement Coefficients (Å^2 × 10^3) for $V_2O_3L_2$

	x	y	z	U(eq)
V(1)	1408(1)	6411(1)	1148(1)	43(1)
O(1)	1365(5)	6596(3)	395(1)	77(1)
O(2)	458(4)	5616(2)	1701(1)	71(1)
O(3)	0	7500	1269(1)	65(2)
O(4)	3383(5)	6682(2)	1343(1)	65(1)
N(1)[b]	2099(8)	4946(5)	765(3)	34(2)
N(2)[b]	2419(9)	4067(5)	1003(3)	40(2)
N(1')[b]	2132(13)	4790(11)	1054(5)	46(3)
N(2')[b]	2622(14)	4250(10)	674(5)	57(4)
C(1)	1980(5)	5921(3)	19(2)	56(1)
C(2)	2429(6)	4928(4)	183(2)	59(1)
C(3)	2979(8)	4195(4)	-191(2)	74(2)
C(4)	3121(7)	4466(4)	-736(2)	71(2)
C(5)	2700(7)	5470(4)	-902(2)	67(2)
C(6)	2114(7)	6200(4)	-529(2)	62(2)
C(7)	1144(6)	4744(3)	1906(2)	52(1)
C(8)	2090(6)	4074(4)	1567(2)	56(1)
C(9)	2749(7)	3128(4)	1773(2)	69(2)
C(10)	2507(8)	2900(4)	2312(2)	76(2)
C(11)	1565(7)	3555(4)	2651(2)	64(1)
C(12)	875(6)	4466(3)	2456(2)	58(1)

[a] Equivalent isotropic U defined as one-third of the trace of the orthogonalized U_{ij} tensor. [b] N(1)(0.6), N(1')(0.4) and N(2)(0.6), N(2')(0.4) correspond to disorder of azo nitrogen atoms (site occupation factors are given in parenetheses) of the type observed before in MnL_2.[2] For clarity only N(1) and N(2) have been shown in Figure 4.

and the activation energy for delocalization is estimated to be only ~3 kcal mol^{-1}.

In order to establish trends and generalities, we are now exploring the valence delocalization phenomenon in other $V_2O_3^{3+}$ complexes electrogenerated from $V_2O_3^{4+}$ congeners of known structures. A second topic under scrutiny is the synthesis of monooxidic mononuclear hexacoordinated species of type VOLD where D is a neutral or monoanionic bidentate coligand which provides an effective handle for controlling the relative stability of the +4 and +5 oxidation states of the metal. The complexes incorporating the $V^{V}O^{3+}$ moiety are of special interest in the context of bromoperoxidase bioinorganic chemistry.[5a,35,36] The results of these investigations will be presented in future papers.

Experimental Section

Materials. $VO(acac)_2$ was prepared as reported.[37] Electrochemically pure dichloromethane, acetonitrile, and tetraethylammonium perchlorate (TEAP) was obtained as before.[38] All other chemicals and solvents were of analytical grade and were used as obtained.

Physical Measurements. Electronic spectra were recorded with a Hitachi 330 spectrophotometer, infrared spectra were taken on a Perkin-Elmer 783 spectrophotometer, and EPR spectra were obtained at X-band on a Varian E-109C spectrometer equipped with a gas-flow temperature controller for variable-temperature studies. A calibrated copper–constantan thermocouple was used to determine sample temperature, and DPPH ($g = 2.0037$) was used to calibrate the spectra. The magnetic moment of $V_2O_3L_2^-$ was determined in dichloromethane solution using the Evans method.[39] The shift of the ^1H signal of CH_2Cl_2 was measured on a Bruker 270-MHz spectrometer at 298 K. Electrochemical measurements were performed on a PAR Model 370-4 electrochemistry system as reported earlier.[40] All potentials reported in this work are uncorrected for junction contribution. Solution (~10^{-3} M) electrical conductivities were measured with the help of a Philips PR 9500 bridge. A Perkin-Elmer 240C elemental analyzer was used to collect microanalytical data (C, H, N).

(35) Vitler, H. *Phytochemistry* **1984**, *23*, 1387–1390.
(36) Arber, J. M.; De Boer, E.; Garner, C. D.; Hasnain, S. S.; Wever, R. *Biochemistry* **1989**, *28*, 7968–7973.
(37) Rowe, R. A.; Jones, M. M. *Inorg. Synth.* **1957**, *5*, 113–116.
(38) Datta, D.; Mascharak, P. K.; Chakravorty, A. *Inorg. Chem.* **1981**, *20*, 1673–1679.
(39) Evans, D. F. *J. Chem. Soc.* **1959**, 2003–2005.
(40) Chandra, S. K.; Basu, P.; Ray, D.; Pal, S.; Chakravorty, A. *Inorg. Chem.* **1990**, *29*, 2423–2428.

Preparation of Compounds. The ligand 2,2′-dihydroxyazobenzene (H_2L) was prepared by reported procedure.[41]

Potassium (2,2′-dihydroxyazobenzenato)dioxovanadate(V), $KVO_2L\cdot1.5H_2O$. To a methanolic solution (20 mL) of H_2L (0.2 g, 0.94 mmol) was added KOH (0.1 g, 1.8 mmol) followed by $VO(acac)_2$ (0.25 g, 0.94 mmol). A red solution was formed that upon evaporation afforded a solid, which was recrystallized from an acetonitrile–benzene (1:1) mixture. Yield: 0.3 g (88.2%). Anal. Calcd for $KVC_{12}H_{11}N_2O_{5.5}$: C, 39.88; H, 3.05; N, 7.75. Found: C, 39.67; H, 2.95; N, 7.62.

Hydroxo(2,2′-dihydroxyazobenzene)oxovanadium(V), VO(OH)L. Through an acetonitrile solution (20 mL) of $KVO_2L\cdot1.5H_2O$ (0.75 g, 2.08 mmol) was passed anhydrous HCl(g) with stirring for 0.5 h, upon which color of the solution changed from red to brown. The solution was then evaporated to dryness, and the dried mass was extracted with benzene. The extract was washed with water to make it acid free. Upon evaporation, a brown solid was obtained. Yield: 0.45 g (73%). Anal. Calcd for $VC_{12}H_9N_2O_4$: C, 48.65; H, 3.04; N, 9.46. Found: C, 48.74; H, 3.16; N, 9.32.

(μ-Oxo)bis[(2,2′-dihydroxyazobenzato)oxovanadium(V)], $V_2O_3L_2$. To a methanolic solution (20 mL) of H_2L (0.2 g, 0.94 mmol) was added 0.25 g (0.94 mmol) of $VO(acac)_2$. The mixture on stirring at room temperature in air for 6 h afforded a deep brown solution which upon evaporation to dryness yielded a solid. It was recrystallized from dichloromethane–hexane (1:1) mixture. Yield: 0.22 g (81.3%). Anal. Calcd for $V_2C_{24}H_{16}N_4O_7$: C, 50.17; H, 2.79; N, 9.76. Found: C, 49.91; H, 2.61; N, 9.58.

Electrosynthesis of $V_2O_3L_2^-$. The following is a representative experiment. A solution of 28.7 mg (0.05 mmol) of $V_2O_3L_2$ in 20 mL of dry dichloromethane (0.1 M TEAP) was reduced coulometrically at a constant potential of 0.0 V vs SCE in nitrogen atmosphere. Electrolysis stopped when 4.72 C had passed. The calculated one-electron coulomb count is 4.82. The reduced solution was used for spectral and magnetic measurements.

Conversion of $KVO_2L\cdot1.5H_2O$ to $V_2O_3L_2$. To an aqueous solution (15 mL) of $KVO_2L\cdot1.5H_2O$ (0.2 g, 0.55 mmol) was added 6 N HCl or $HClO_4$ dropwise. This resulted in immediate precipitation of a deep brown solid. Addition of acid was continued until precipitation was complete. The solid was collected by filtration, washed thoroughly with water, and then dried in vacuo over P_4O_{10}. Yield: 0.13 g (81.7%).

Conversion of $V_2O_3L_2$ to $KVO_2L\cdot1.5H_2O$. To a methanolic solution (15 mL) of $V_2O_3L_2$ (0.25 g, 0.44 mmol) was added KOH (0.05 g, 0.89 mmol). The color of the solution changed from brown to red. The mixture was stirred at room temperature for 1 h, and upon evaporation the required complex was obtained in 91.4% yield (0.29 g).

Conversion of VO(OH)L to $V_2O_3L_2$. A 0.2-g sample (0.68 mmol) of VO(OH)L dissolved in 15 mL of dry dichloromethane was allowed to stand in a stoppered flask. After a few days brown shining crystals were isolated. These were found to have the same spectral properties as those of $V_2O_3L_2$. Yield: 0.165 g (85%).

X-ray Structure Determination. A single crystal of $V_2O_3L_2$ (0.30 × 0.26 × 0.38 mm^3) grown by slow diffusion of hexane into a dichloromethane solution and a single crystal of $KVO_2L\cdot1.5H_2O$ (0.20 × 0.24 × 0.32 mm^3) grown by slow diffusion of an acetonitrile solution into benzene were used. In both cases the cell parameters were determined by a least-squares fit of 30 machine-centered reflections (2θ = 15–30°). Data were collected by the ω-scan method in the 2θ range 2–55° (for both) on a Nicolet R3m/V diffractometer with graphite-monochromated Mo Kα radiation (λ = 0.710 73 Å). Two check reflections measured after every 98 reflections for both complexes showed no significant intensity reduction during the 58 h ($V_2O_3L_2$) and 112 h ($KVO_2L\cdot1.5H_2O$) of exposure to X-rays. Data were corrected for Lorentz–polarization effects, and empirical absorption corrections were done for both complexes on the basis of azimuthal scans of six reflections.[42] Systematic absences led to the identification of the space group as *Pcnb* for $V_2O_3L_2$ and *Cc* or *C2/c* for $KVO_2L\cdot1.5H_2O$. The structure of the latter complex was successfully solved in the *C2/c* space group. For $V_2O_3L_2$, 3082 reflections were collected, 2263 were unique, and 1402 satisfying $I > 3.0\sigma(I)$ were used for structure solution. In the case of $KVO_2L\cdot1.5H_2O$ the corresponding numbers are 7145, 6492, and 4224, respectively.

All calculations for data reduction, structure solution, and refinement were done on a MicroVAX II computer with the programs of SHELXTL-PLUS.[43] Both structures were solved by direct methods and refined by full-matrix least-squares procedures making all non-hydrogen atoms anisotropic. Hydrogen atoms were included in calculated positions with fixed U (=0.08 $Å^2$). The highest difference Fourier peaks were 0.21 and 0.18 e/$Å^3$ for $V_2O_3L_2$ and $KVO_2L\cdot1.5H_2O$, respectively. Significant crystal data are listed in Table IV, and atomic coordinates and isotropic thermal parameters are collected in Tables V and VI.

Acknowledgment. Financial support received from the Department of Science and Technology, New Delhi, and Council of Scientific and Industrial Research, New Delhi, is gratefully acknowledged.

Supplementary Material Available: Tables SI–SVIII, listing anisotropic thermal parameters, complete bond distances and angles, and hydrogen atom positional parameters (10 pages). Ordering information is given on any current masthead page.

(41) Drew, H. D. K.; Landquist, J. K. *J. Chem. Soc.* **1938**, 292–304.
(42) North, A. C. T.; Philips, D. C.; Mathews, F. S. *Acta Crystallogr., Sect. A* **1968**, *24*, 351–359.
(43) Sheldrick, G. M. *SHELXTL-PLUS 88, Structure Determination Software Programs*; Nicolet Instrument Corp.; Madison, WI, 1988.